

# Ocean Circulation Hindcast at the Brazilian Equatorial Margin

Luiz Paulo de Freitas Assad<sup>2</sup>, Raquel Toste<sup>1</sup>, Carina Stefoni Böck<sup>1</sup> Dyellen Soares Queiroz<sup>3</sup>, Anne Goni Guedes<sup>3</sup>, Maria Eduarda Pessoa<sup>3</sup> and Luiz Landau<sup>1</sup>

<sup>1</sup> Laboratório de Métodos Computacionais em Engenharia, LAMCE/COPPE/UFRJ Av. Athos da Silveira Ramos, 149, Centro de Tecnologia – Bloco I – Sala 214  
Cidade Universitária, Rio de Janeiro – RJ, Brazil - 21941-999

<sup>2</sup> Departamento de Meteorologia  
Av. Athos da Silveira Ramos, 149, Centro de Tecnologia – Bloco I – Sala 214  
Cidade Universitária, Rio de Janeiro – RJ, Brazil - 21941-999

<sup>3</sup> Enauta (Queiroz Galvão Exploração e Produção S.A.)  
Avenida Almirante Barroso, 52, Centro, Rio de Janeiro – RJ

**Abstract.** The growth of the activities of the Petroleum Industry in the Brazilian Equatorial Margin, reinforces the need for the environmental knowledge of the region, which will be potentially exposed to risks related to such activities. The environmental importance of this region evidences the need to deepen and systematize not only the knowledge about the environmental sensitivity of the region, but also about the characteristics that will exert influence over it. The Costa Norte Project can be identified with one of these initiatives. The project has as one of the main objectives to evaluate the efficiency of the use of marine hydrodynamic environmental computational modeling methods to represent the marine dynamics over that region. In this paper a regional ocean computational model was used to produce an inedited ten year hindcast simulation in order to represent the main aspects associated with mesoscale climatological ocean circulation at the Brazilian equatorial margin. This article aims to present the methodology and the results analysis and evaluation associated to the cited hydrodynamic computational simulation. The obtained results clearly demonstrated the ocean model potential to represent the most important ocean variables space and time distribution over the studied region. Comparative analysis with observed data demonstrated good agreement with temperature, salinity and sea surface height fields generated by the implemented model. The Costa Norte Project is carrying out under the Brazilian National Petroleum Agency (ANP) R&D levy as “Investment Commitment to Research and Development” and is financially supported by Enauta O&G company.

**Keywords:** Ocean Modelling, Regional Ocean Circulation, Climatological Hindcast, Brazilian Equatorial Margin, Costa Norte Project.

## 1. Introduction

The growth of the activities of the Petroleum Industry in the Brazilian Equatorial Margin, reinforces the need for ocean circulation knowledge of the region, which will be exposed to greater risks of environmental impacts related to such activities. Potential oil spill accidents associated with these activities would bring several environmental damages for that region. The nature of this vast region in terms of the magnitude of energy forcing (currents, tides, waves and winds) coupled with the high local biological wealth, both in terms of species and ecosystems makes several sectors of society turn their attention to potential activities to be implemented in this area. It stands out, from the environmental point of view, the presence of what are considered the largest areas of mangroves on the planet (Souza Filho et al., 2005).

All this environmental particularity evidences the need to deepen and systematize not only the knowledge about the environmental sensitivity of the region, but also about the characteristics that will exert influence in the operations of the oil industry and contingency actions in case of eventual accidents. The Costa Norte Project can be identified with one of these initiatives. Financially supported by Enauta O&G company, the project has as one of the main objectives to evaluate the efficiency of the use of marine hydrodynamic environmental computational modeling methods to represent the marine dynamics, particularly in the region that includes some marine sedimentary basins the estuaries of Amazon and Pará rivers. It should be noted that the aforementioned project is carry out under the Brazilian National Petroleum Agency (ANP) R&D levy as “Investment Commitment to Research and Development”.

In this paper a regional ocean computational model was used to proceed with an inedited ten year hindcast simulation in order to represent the main aspects associated with mesoscale ocean circulation at the Brazilian equatorial margin. This article aims to present the methodology and the results analysis associated to the cited hydrodynamic computational simulation. An evaluation of the results obtained with the simulation will also be presented based on the comparisons of some ocean variables produced by the model and remote and in situ data sets available for the study region. It is important to emphasize that the presented development corresponds to a first step towards the implementation of an operational regional ocean model for the Equatorial Brazilian Margin.

## 2. Study Area

In this section it will be described a brief overview about the main aspects associated ocean dynamics near the Brazilian equatorial margin. There are, four main ocean dynamics forcing's at the studied region: The North Brazil Current flow, tides, amazon river discharge and trade winds (Figure 1).

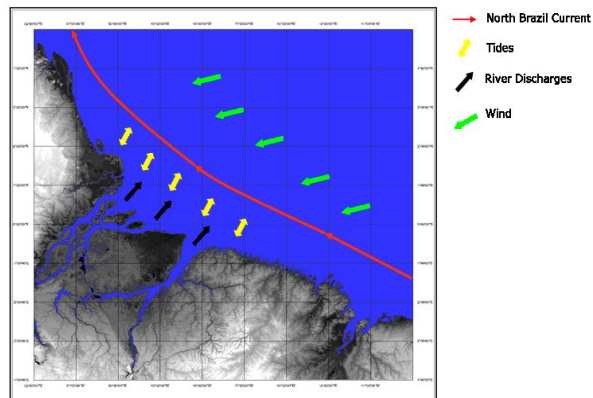


Fig 1. Schematic representation of the main environmental forcing to Amazon Continental Shelf ocean dynamics.

The atmospheric circulation in this region is dominated by trade winds, with the strongest season from December to April and winds from the Northeast direction (Geyer et al, 1996). Ocean dynamics has strong annual and interannual variability related to local and remote influence of atmospheric processes with distinct spatial scales. The North Brazil Current (NBC) represents the main influence for the marine circulation in a regional scale. The NBC is a strong western boundary ocean current originated from the South Equatorial Current (SEC) (Geyer et al, 1996; Nittrouer & DeMaster, 1996), and influences Amazon River plume transport (Limburner et al, 1995). Also, NBC closes the equatorial ocean circulation gyre generated by the wind. It also feeds the North Equatorial Counter Current (NECC) (Johns et al, 1998). The Amazon River discharge is also an important contributor to Amazon Continental Shelf hydrodynamics. Its average discharge is  $180,000\text{m}^3/\text{s}$  which represents around 16% of the global river discharge into the oceans and its seasonality is associated with Andes freezing processes with minimum discharge in November and maximum in May (Geyer et al, 1996). The continental shelf has its circulation strongly influenced by the tides. The region is dominated by a macrotidal regime with variations of up to 8 meters. The tides have semidiurnal periodicity. It is important to emphasize the all of these environmental forcing act in different time and spatial scales at the equatorial margin ocean dynamics.

### 3. Methodology

In this section, information will be presented regarding the computational hydrodynamic model, the boundary and initial conditions used as well as details regarding the methodology of analysis and evaluation of the obtained results.

### 3.1 The Hydrodynamic Model

The numerical model to be used is the Regional Ocean Modeling System (ROMS) (Shchepetkin & McWilliams, 2005). The ROMS is a free surface model that solves the primitive equations of the oceans in a Arakawa C-grid, through a system of curvilinear horizontal coordinates. This system allows the grid to be defined along the coastline, which allows different resolutions in the contours of the grid and favors the observation of flows close to the coastal contours (Hedstrom, 2012).

#### The Numerical grid

The generated numerical grid is comprised between latitudes  $11.95^{\circ}$  N and  $5.45^{\circ}$  S and between longitudes  $55.95^{\circ}$  W and  $35.54^{\circ}$  W. It is composed of  $246 \times 210$  cells, which represents the horizontal resolution of  $1 / 12^{\circ}$  (Figure 2). The numerical grid has 30 vertical levels. In Figure 2, it is represented the numerical grid domain and the bathymetry field used by the model.

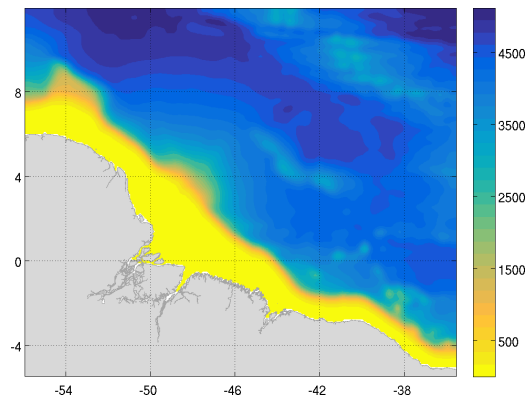


Fig 2. Numerical grid domain and the bathymetry field used by the model simulation.

The model was forced (used as boundary conditions) by three of the main ocean dynamic forcing described on section 2 that are winds, river discharge and the NBC flow. The model also used as initial conditions the mass field of the study area represented by the temperature and salinity fields.

### 3.2 Initial and Boundary Ocean Conditions

It was acquired daily mean ocean velocity (meridional and zonal), mass (temperature and salinity) and sea surface height fields from the Copernicus Marine Environment Monitoring Service (CMEMS) with  $1/12^{\circ}$  horizontal resolution with 40 vertical levels for the simulation period. This data set was processed and used as initial and boundary ocean conditions for the implemented model. In figure 3 it is represented the

current field over the sea surface temperature field (Figure 3) and the sea surface velocity field (Figure 3) used as initial conditions for the hindcast simulation.

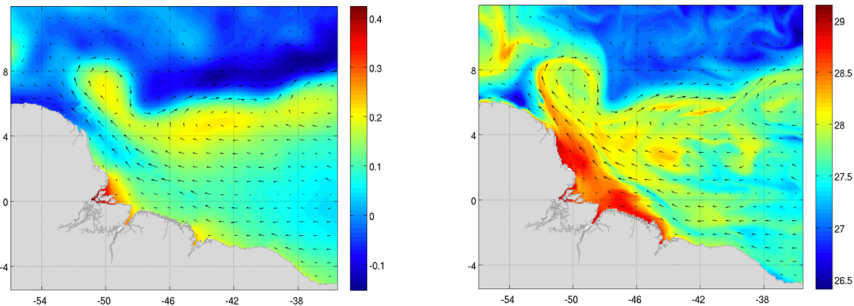


Fig 3. Sea surface current field over the velocity distribution (left) and sea surface temperature field (right) used as initial conditions. The data were acquired from CMEMS.

### River Discharge

The climatological river discharge time series used as boundary conditions by the ocean regional model were obtained for three rivers: Amazon, Tocantins and Pindaré (Figure 4). The climatologies for Amazon and Pindaré river were estimated from river discharge time series acquired from HYBAM and international research laboratory and Brazilian National Water Agency respectively. The climatology for Tocantins river discharge was the same that one presented by Nikiema et al. (2007).

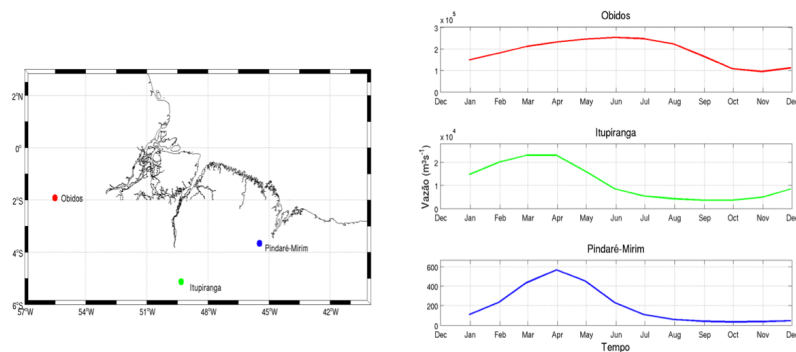


Fig 4. River discharge station sites (left) and river discharge time series plot for each site.

### 3.2 Atmospheric Boundary Conditions

It was acquired the datasets from Reanalysis 2 project from National Centers of Environmental Prediction (Kalnay et al., 1996; Kanamitsu et al., 2002), with space res-

olution of  $2^\circ$  and time resolution of 6 hours for the entire simulation period. The acquired data correspond to the zonal and meridional wind stress field (Figure 5). It was also acquired the heat and mass fluxes over the sea surface (not shown).

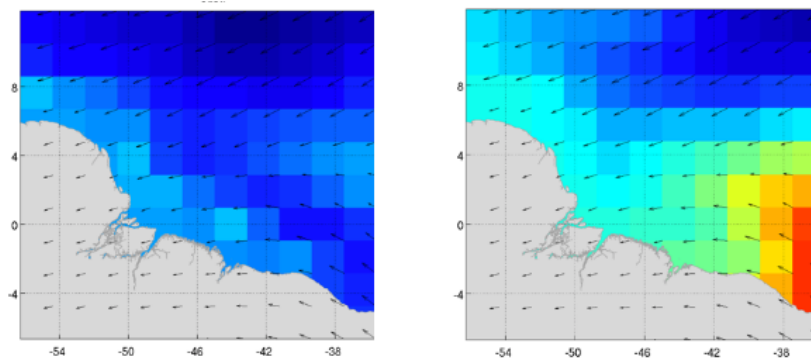


Fig 5. Average wind stress field (N.m-2) for the year of 2007. On left it is represented the zonal component of the wind stress field and on the right the meridional component of the wind stress field. The vectors indicate the resultant direction of the wind.

### 3.4 Model Evaluation

The results of the simulations were compared with remote and *in situ* data observations, considering the variables sea surface temperature, salinity and sea surface height. These comparisons were made in order to evaluate the ocean model skill in obtain a consistent climatological regional ocean representation of the study region. The databases acquired and used in each of the analyzes will be described below. The conducted analysis will be also described at the end of this section.

#### PIRATA Project

The Prediction and Research Moored Array in the Tropical Atlantic (PIRATA) project is a multinational cooperation program between Brazil, France and the United States, initiated in 1977, in which the three countries share the tasks of implementing and maintaining the observation network (Servain et al., 1998, Burles et al., 2008, GOOS, 2017). The project corresponds to an *in situ* observation network composed of meteoceanographic buoys designed to monitor several variables of the ocean-atmosphere interaction processes in the tropical Atlantic Ocean region (GOOS, 2017). Among others, the measured variables include temperature and salinity of the sea surface (Servain et al., 1998; GOOS, 2017), which were used for comparison with the simulations. Only three buoys are located within the numerical grid used in the simulations and their locations are shown in Figure 6.

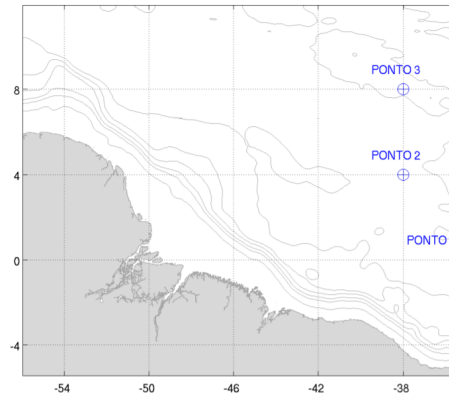


Fig 6. Location of the PIRATA buoys used for evaluation analysis superimposed on the bathymetry field of the study area.

### Advanced Very High Resolution Radiometer

The Advanced Very High Resolution Radiometer (AVHRR) (Price, 1984). With  $0.05^\circ$  resolution, the mesoscale oceanic features are well captured by this data base. The comparison with this base was done by analyzing the surface fields and time series extracted at four points of the numerical grid as shown in Figure 7. These points were chosen in order to obtain a representative analysis of the different areas in the numerical grid. This evaluation is important in order to observe not only the temporal but also the spatial patterns of temperature variation.

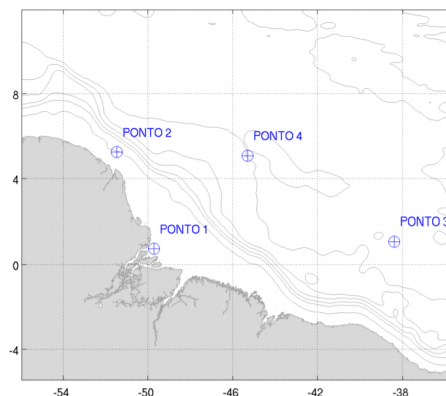


Fig 7. Localization of the points used to extract the time series of SST.

### AVISO project

Passive microwave sensors use the backscatter of electromagnetic waves on the surface of the sea and thus obtain remote information even with the presence of clouds, which makes the mesh of estimates more homogeneous. The altimeter is an example of this type of passive sensor; through the return time of a pulse emitted vertically from

the location, the sensor is able to measure the height of the sea surface in relation to its already known position. In this way, it is possible to estimate the height of the sea surface in relation to the terrestrial geoid. More specifically, the sea surface anomaly, which was used to compare the simulations, is deduced from the height of the sea surface with a resolution of  $0.25^\circ$ . The anomaly data were obtained through the French database Archiving, Validation and Interpretation of Satellite Oceanographic data (AVISO). As for SST, the sea surface height was also evaluated in the four points shown in Figure 7.

### 3.5 Evaluation Analysis

The analysis of the results of the climatological round was performed using the bases described in the previous item, for sea surface temperature, sea surface height and salinity. Basically, the analyzes were performed considering the bias and the mean square error (RMSE), calculated according to Equations 1 and 2.

$$bias = y_t^{mod} - y_t^{obs} \quad (1)$$

$$RMSE = \sqrt{\frac{1}{N} \sum_{t=1}^N (y_t^{obs} - y_t^{mod})^2} \quad (2)$$

where  $t$  is time,  $N$  is the number of observations,  $y_t^{obs}$  is the observation e  $y_t^{mod}$  is the model result.

## 4. Results

### 4.1 The Hindcast Simulation

After the preprocessing of the initial and boundary conditions the model was integrated for a long period of ten years from December 27, 2006 to June 30, 2017. The choice of this period is justified because it corresponded to the period in which all bases used as boundary conditions were available. The simulation was performed for the mentioned period, considering an internal time step of 600 s and an external time step of 20s. The results for the period prior to January 2007 were discarded. In Figure 8 the kinetic energy time series plot is presented, and it is possible to verify that the model adjustment is found quickly achieved, at the beginning of the simulation. This behavior is consistent since the fields used as initial and boundary conditions have the same spatial resolution as the regional grid used in this step.

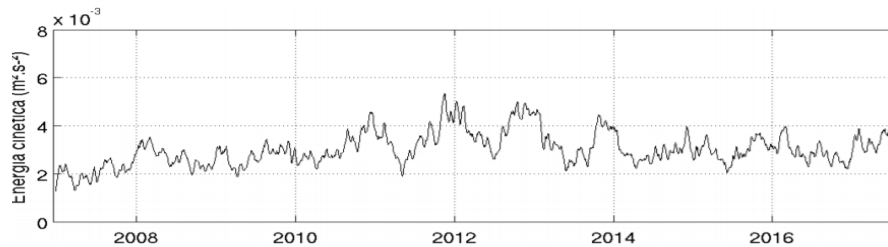


Fig 8. Average kinetic energy time series plot integrated for the entire grid region for the period from December 27, 2006 to June 30, 2017.

## 4.2 Analysis

### Sea Surface Temperature - AVHRR

For the evaluation of the SST generated by the model the equations presented in section 3 were applied with the data of the AVHRR sensor for the points showed in Figure 7. Figure 9 shows the time series plot of the model's SST and the AVHRR data (top panel) and the bias between the two series (lower panel) referring to Point 1. It is observed that the model overestimates the temperature values at different times in the series, cyclically, with anomalies above  $2^{\circ}\text{C}$  and in some instants reaching  $4^{\circ}\text{C}$ . Meanwhile, the average of the bias is approximately  $1.0^{\circ}\text{C}$ . It is important to note that Point 1 is located in the region of the mouth of the Amazon River, where there is intense variability, which may contribute to the greatest differences.

Point 2 (Figure 10) does not exhibit the same behavior as Point 1 and the model and data series tend to exhibit the same behavior. Thus, the bias presents smaller and average values of approximately  $-0.2^{\circ}\text{C}$ , that is, in general, there is an underestimation in the SST. In contrast to what happens in Point 1, Point 2 is located in a region whose dynamics is most behaved and dominated by the Northern Current of Brazil (Johns et al., 1990).

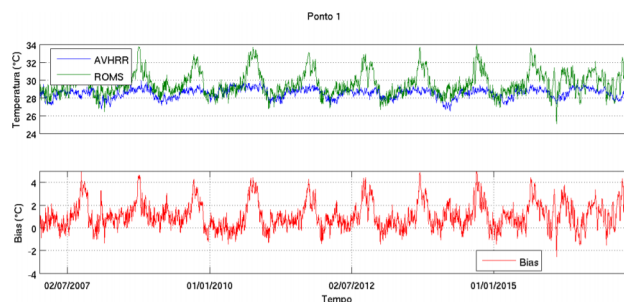


Fig 9. Time series plot of SST (upper panel) and bias (lower panel) between model and AVHRR sensor data in Point 1.

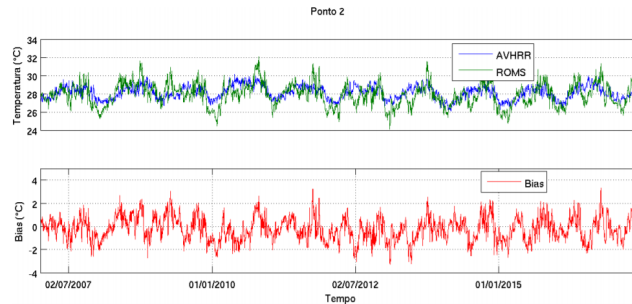


Fig 10. Time series plot of SST (top panel) and bias (bottom panel) between model and AVHRR sensor data in Point 2.

In Point 3 (not shown), little variability is observed in the SST from the AVHRR data, with the temperature oscillating around 28 °C. The model, however, captured greater variability. In general, there was an underestimation of SST by the average model of -0.9°C. In Point 4 (not shown) the two series exhibit similar cyclic behavior, which indicates that the climatology is satisfactorily representing the features of that region. Despite the differences between the two series over time, especially in the representation of the minimum temperatures, the average value of the bias was -1.2° C, which still shows a good correlation between the two series.

#### Sea Surface Temperature - PIRATA

The same evaluation conducted with AVHRR data was done with the PIRATA data. The surface temperature data of the three buoys located in the study area (Figure 6) were compared with the time series generated by the model at the nearest grid points. Figure 11 shows the time series plots of SST of the climatological model and PIRATA in the upper panel, and the bias between the two series, in the lower panel, obtained for Point 1. Several intervals of time are observed with no data recorded on this PIRATA buoy, and the same occurs on the other buoys located in Points 2 and 3. A good agreement between the modeled values and the PIRATA data is observed, which can also be verified by the low values of bias throughout the series.

At point 2 (not shown), which has larger sample gaps, larger differences are observed between the modeled and observed values than at Point 1. Despite this, the bias does not exceed mean values of -0.7 °C, indicating a good correlation between them. The time series of Point 3 (not shown) is, among others, the one with the greatest differences, and for the most part, the climatological model underestimates the maximum temperatures and overestimates the minimum ones. Nevertheless, as in Point 2, on average, the difference between the two series is -0.97 °C, also indicating a good correlation between them.

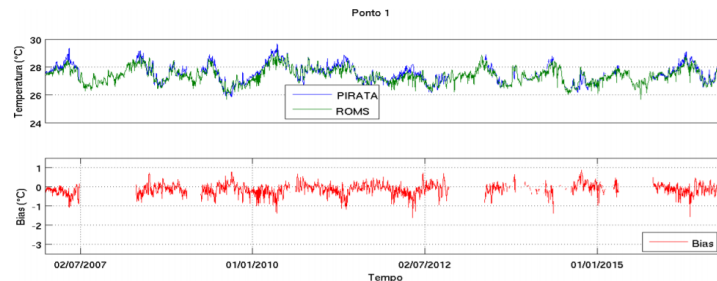


Fig 11. Time series plots of the surface temperature (top panel) and bias (bottom panel) between the model results and the PIRATA Project data in Point 1, in degrees Celsius.

### Salinity

For the analyzed period, as well as for temperature, gaps were observed in the measurement of salinity in the three PIRATA buoys. In spite of this, it is possible to verify that the model adequately represented surface salinity, especially in the float located in Point 1 (Figure 12). In Point 2 and in Point 3 (not shown), errors were observed in the representation of the peaks of lower salinities. However, overall, there is a good representation of seasonality in Point 3.

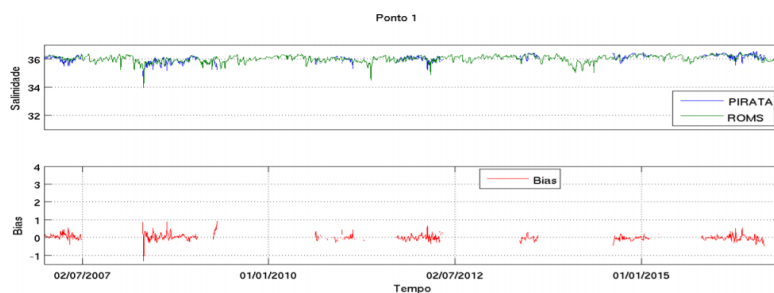


Fig 12. Time series of salinity on the surface (top panel) and bias (bottom panel) between the model result and the data from the Point 1 PIRATA Project

### Sea Surface Height

The comparison of the free surface elevation between the climatology generated by ROMS and the AVISO database was performed in two stages. The first one consisted in quantifying the time variance of the sea level anomaly at each point of the numerical grid, representing the turbulent variability. The second stage consisted in extracting time series from the sea surface anomaly at the sampling points shown in Figure 3, located in the region of interest.

Figure 13a represents the horizontal variance field of the sea surface anomaly estimated from the AVISO data. There is little variability, with the exception of the coastal region of Amapá and part of the Amazon River mouth region, which present higher values of variance. Although it is a region of greater variability, the highest values of variance do not exceed 0.14 m. On the basis of the variance calculated from the results of the model run, this higher variability is not observed near Amapá, and the highest values are found in the internal region of the mouth of the Amazon River (Figure 13b). This difference is most clearly observed through the bias between the fields

(Figure 13c), whose highest values lie precisely in the regions of greater variance of the AVISO data base. Nevertheless, similar features occur in the oceanic region (Figure 13), where a range of greater variability is observed in the internal region of retroflexion of the Northern Brazil Current and in the region of formation and detachment of vortices.

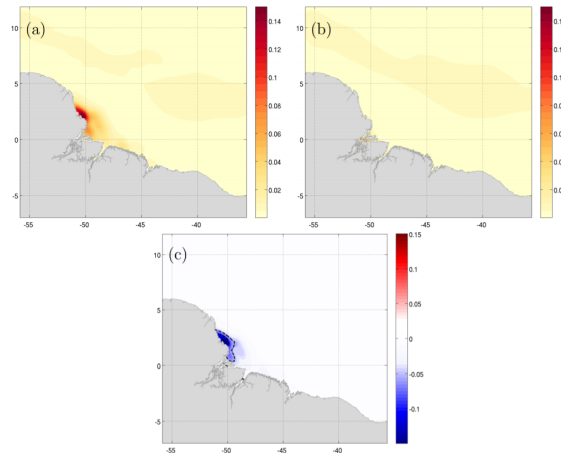


Fig 14. Mean variance field of the sea surface anomaly, from 2007 to 2016, referring to the database of AVISO (a), the climatology generated by ROMS (b) and the bias between the two fields (c), in  $m^2$ .

Figure 15 shows the series extracted from the climatological results generated by the ROMS and the AVISO fields in Point 1. The greatest variability at this point is observed for the AVISO when compared to the model results, which is reflected in higher values of bias, which for the most part ranges from -0.5 to 1.0 m. It should be noted that Point 1 is very close to the region of greatest variability found in Figure 63a, which also explains the differences found.

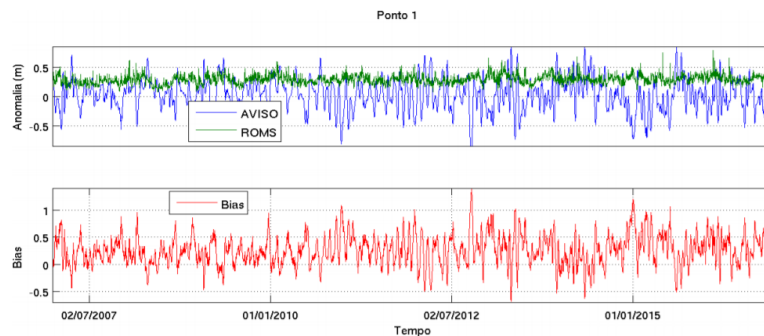


Fig 15. SSH anomaly mean variance time series plot (top panel) and bias (bottom panel) between the model and the AVISO data in Point 1, in meters.

For point 2 (Figure 16), the values of bias are very close to zero and the variability of the series is expressively smaller. By verifying the location of these points (Figure 7) in relation to the variability fields shown in Figures 14a and 14b, it is noted that these are located in regions of low variability, both when considering the modeled results and the AVISO observation data. In spite of this low variability, the climatology generated by the ROMS presents a very similar behavior to the data of the base AVISO in these points, where it is possible to observe that the model captured the cyclic oscillation behavior of the sea level, evidenced mainly through the time series in Point 3 (not shown).

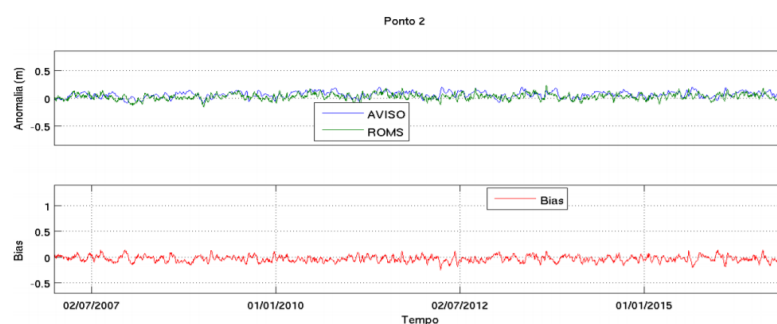


Figure 16. Time series plot of the sea surface anomaly (top panel) and bias (bottom panel) between the model and the AVISO data in Point 2, in meters.

## 5. Conclusions

A regional ocean computational model was implemented and executed in order to obtain an inedited ten-year climatological ocean hindcast for the Brazilian equatorial margin. From the conducted evaluation analysis, it was verified that the model adequately represented the main ocean variables distribution in the study region. The SST, salinity and SSH fields generated by the model presented consistent results in offshore regions of the study area and less consistent results in coastal areas. The results indicated that the produced hindcast could be an important source of information for climatological studies related with NBC and other mesoscale oceanographic processes in the Brazilian Equatorial Margin. It is important to emphasize that the presented development corresponds to a first step towards the implementation of an operational regional ocean model using data assimilation techniques for the study region.

## 6. References

Argo Science Team, 2000, Report of the Argo Science Team 2nd Meeting (AST-2) March 7–9, 2000, Southampton Oceanography Centre, Southampton, U.K.

- Geyer, W. R., Beardsley, R. C., Lentz, S. J., Candela, J., Limeburner, R., Johns, W. E., Castro, B. M. and Soares, I. D., 1996. Physical oceanography of the Amazon shelf, *Continental Shelf Research*, 16 (5/6), 575 – 616.
- GOOS, 2017. GOOS-Brasil. Aliança Regional para a Oceanografia no Atlântico Sudoeste Superior e Tropical – OCEATLAN.
- Johns, W.E., Lee, T.N. Schott, F.A. Zantopp, R.J., Evans, R.H., 1990, The North Brazil Current retroflection: Seasonal structure and eddy variability. *J. Geophys. Res.*, v. 95, n. C12, pp. 2156-2202.
- Kalnay E., Kanamitsu M., Kistler R., Collins W., Deaven D., Gandin L., Iredell M., Saha S., White G., Woollen J., Zhu Y., Leetmaa A., Reynolds R., Chelliah M., Ebisuzaki W., Higgins W., Janowiak J., Mo K.C., Ropelewski C., Wang J., Jenne R., Joseph D., 1996, The NCEP/NCAR 40-Year Reanalysis Project. *Bull. Amer. Meteor. Soc.*, v. 77, n. 1, pp. 437–471.
- Kanamitsu, M., Ebisuzaki, W., Woollen, J., Yang, S.-K., Hnilo, J.J., Fiorino, M., Potter, G.L., 2002, NCEP-DOE AMIP-II Reanalysis (R-2). *Bulletin of the American Meteorological Society*, v. 83, n. 1, pp. 1631-1643.
- Limeburner, R., Beardsley, R. C., Soares, I. D., Lentz, S. J., Candela, J., 1995. Lagrangian flow observations of the Amazon River discharge in the North Atlantic. *Journal of Geophysical Research*, 100 (C2), 2401-2415.
- Nikiema, O., Devenona, J., Bakloutib, M., 2007, Numerical modeling of the Amazon River plume. *Continental Shelf Research*, v. 27, n. 1, pp.873–899.
- Nittrouer, C. A. and DeMaster, D. J., 1996. The Amazon shelf setting: tropical, energetic, and influenced by a large river. *Continental Shelf Research*, 16 (5/6), 553 – 573.
- Oka, E., Ando, K., 2004, Stability of Temperature and Conductivity Sensors of Argo Profiling Floats. *Journal of Oceanography*, v. 60, n. 2, pp. 253-258.
- Price, J.C., 1984, Land Surface Temperature Measurements From the Split Window Channels of the NOAA 7 Advanced Very High Resolution Radiometer. *J. Geophys. Res.*, v. 89, pp. 7231-7237.
- Roemmich, D.H., Davis, R.E., Riser, S.C., Owens, W.B., Molinari, R.L., Garzoli, S.L., Johnson, G.C., 2003, The Argo Project. *Global Ocean Observations for Understanding and Prediction of Climate Variability*. Technical Report - Scripps Institution of Oceanography, La Jolla CA., 9p.
- Shepetchkin, A.F., McWickiams, J.C., 2005, The regional oceanic modeling system (ROMS): a split-explicit, free-surface, topography-following-coordinate oceanic model. *Ocean Modelling*, v. 9, pp. 347–404.
- Servain, J., Busalacchi, A.J., McPhaden, M.J., Moura, A.D., Reverdin, G., Vianna, M., Zebiak, S.E., 1998, A Pilot Research Moored Array in the Tropical Atlantic (PIRATA). *Bull. Amer. Meteor. Soc.*, v. 79, pp. 2019–2031.
- Souza Filho, Pedro Walfir Martins. (2005). Costa de manguezais de macromaré da Amazônia: cenários morfológicos, mapeamento e quantificação de áreas usando dados de sensores remotos. *Revista Brasileira de Geofísica*, 23(4), 427-435.